# Tissue engineering of the tympanic membrane using electrospun PEOT/PBT copolymer scaffolds

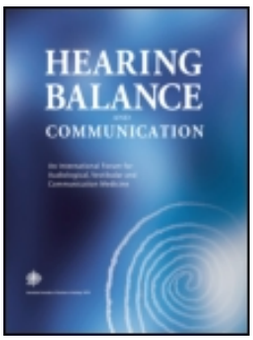

Hearing, Balance and Communication

ISSN: 2169-5717 (Print) 2169-5725 (Online) Journal homepage: http://www.tandfonline.com/loi/ihbc20

# Tissue engineering of the tympanic membrane using electrospun PEOT/PBT copolymer scaffolds: A morphological in vitro study

**Serena Danti, Carlos Mota, Delfo D'alessandro, Luisa Trombi, Claudio Ricci, Sharon L. Redmond, Andrea De Vito, Roberto Pini, Rodney J. Dilley, Lorenzo Moroni & Stefano Berrettini**

**To cite this article:** Serena Danti, Carlos Mota, Delfo D'alessandro, Luisa Trombi, Claudio Ricci, Sharon L. Redmond, Andrea De Vito, Roberto Pini, Rodney J. Dilley, Lorenzo Moroni & Stefano Berrettini (2015) Tissue engineering of the tympanic membrane using electrospun PEOT/PBT copolymer scaffolds: A morphological in vitro study, Hearing, Balance and Communication, 13:4, 133-147, DOI: 10.3109/21695717.2015.1092372

**To link to this article:** http://dx.doi.org/10.3109/21695717.2015.1092372

Published online: 12 Oct 2015.

*Hearing, Balance and Communication*, 2015; 13: 133–147

Taylor & Francis
Taylor & Francis Group

**ORIGINAL ARTICLE**

# Tissue engineering of the tympanic membrane using electrospun PEOT/PBT copolymer scaffolds: A morphological in vitro study

SERENA DANTI[1,2], CARLOS MOTA[2,3], DELFO D'ALESSANDRO[1,2], LUISA TROMBI[2], CLAUDIO RICCI[2], SHARON L. REDMOND[4], ANDREA DE VITO[2], ROBERTO PINI[5], RODNEY J. DILLEY[4], LORENZO MORONI[3] & STEFANO BERRETTINI[1,2]

*[1]Department of Surgical, Medical, Molecular Pathology and Emergency Medicine, University of Pisa, Pisa, [2]Laboratory of Temporal Bone Dissection and Otologic Tissue Engineering (OtoLab), Azienda Ospedaliero-Universitaria Pisana, Pisa, Italy, [3]Institute for Technology Inspired Regenerative Medicine (MERLN), Complex Tissue Regeneration Department, Maastricht University, Maastricht, The Netherlands, [4]Ear Science Institute Australia and Ear Sciences Centre, School of Surgery, University of Western Australia, Nedlands, Australia, and [5]Institute of Ecosystem Study (ISE), National Research Council (CNR), Pisa, Italy*



**Abstract**

*Objective*: Tissue engineering has recently been identified as a suitable tool to develop replacements for the tympanic membrane. This study aimed at investigating PEOT/PBT copolymer scaffolds obtained via electrospinning as potential eardrum substitutes using an in vitro approach. *Study design*: PEOT/PBT copolymer ultrafine fibre meshes were manufactured and characterized for morphology and pore features. The scaffolds were cultured with human mesenchymal stromal cells (MSCs) under a dynamic flow regimen to improve cell infiltration and viability. The expression of basic extracellular matrix molecules was evaluated and compared to that of the human eardrum. Finally, the interaction between human tympanic membrane keratinocytes and the scaffolds was investigated. *Results*: The electrospun scaffolds had a fibre diameter of $1.9 \pm 0.9\,\mu m$, thickness of $220 \pm 56\,\mu m$, and porosity of $80\% \pm 0.8\%$. The macroporous meshes were suitable for cell infiltration, since 83.3% of relative void volume was from pores of 3–300-μm size. Over a four week culture, the bioreactor always increased the viability of human MSCs in the scaffolds with respect to traditional multi-well plate cultures. Viability was best at two weeks in culture, so this time-point was selected for further morphological and histochemical analyses. In static cultures, the human MSCs interacted with the top surface of the fibrous scaffold, while in dynamic cultures they infiltrated the mesh up to 240-μm depth. Adherent human MSCs maintained a non-differentiated phenotype, as shown by a very low production of glycosaminoglycans and glycoproteins, which are conversely highly expressed in the eardrum connective tissue layer. Human tympanic membrane keratinocytes adhered to the scaffold surface and were viable after 48 h. *Conclusion*: Using electrospinning combined with bioreactor culture appeared an efficient approach to develop biohybrid eardrum replacements in vitro, suitable for re-epithelialization in vivo.

**Key words:** *electrospinning*, *mesenchymal stromal cells (MSCs)*, *tissue engineering*, *eardrum*, *keratinocytes*

## Introduction

The eardrum, or tympanic membrane (TM), is a thin and tough tissue separating the outer from the middle ear compartments. It collects and transmits sound waves to the ossicular chain. From a histological and functional standpoint, the human TM is composed of two different areas, the pars tensa and the pars flaccida. In cross sections, the eardrum shows a trilaminar structure: a fibrous mid-layer or lamina propria, and epidermal or mucosal epithelia as covering layers on the other sides (Figure 1). In specific areas, the human TM ranges in thickness from 20 to 100 μm (1,2). Several pathologies may damage this tissue, such as otitis media, tympanosclerosis, cholesteatoma and perforation (3,4). The latter represents a widespread clinical problem, usually caused by trauma or infection. TM perforations occur with the highest prevalence in

Correspondence: S. Berrettini and S. Danti, Department of Surgical, Medical, Molecular Pathology and Emergency Medicine, University of Pisa, Pisa, Italy. E-mail: s.berrettini@med.unipi.it and s.danti@med.unipi.it

*(accepted 7 September 2015)*

ISSN 2169-5717 print/ISSN 2169-5725 online 
DOI: 10.3109/21695717.2015.1092372

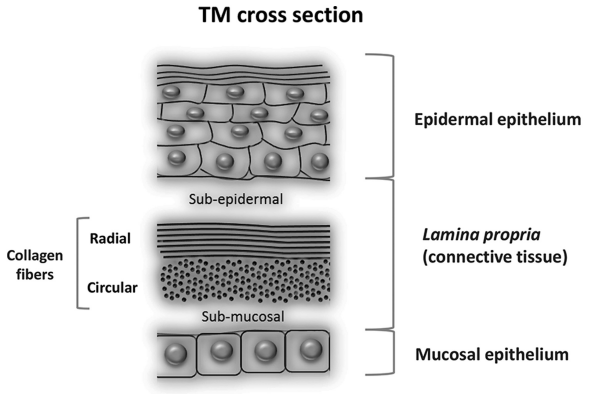


Figure 1. Schematic drawing of a cross-sectioned tympanic membrane, showing the tri-laminar structure of the pars tensa as depicted by Lim (1).

childhood and show ethnicity dependence (4,5). Even though most perforations can heal spontaneously, there are issues deserving clinical attention. For example, chronic infections deriving from perforations can lead to conductive hearing loss, secondary infection, squamous epithelial cysts, and cholesteatoma formation, eventually requiring surgical management (4,6,7). Moreover, since epithelia drive TM closure spontaneously, the fibrous mid-layer in the neo-formed tissue is missing in some patients. As a result of this morbidity, the TM has sub-optimal function and is sensitive to re-perforation.

Current surgical techniques for the treatment of TM perforations include myringoplasty or tympanoplasty, the latter for perforations associated with middle ear pathology. In small perforations, fat, paper or other patches are applied to induce self-repair, while in large perforations, connective tissue grafts, such as tragal cartilage, muscle fascia and perichondrium, are used to replace the eardrum (8–10). To date, the autologous temporalis fascia is considered the gold standard material for TM reconstruction (8). However, some patients have limited graft availability, such as in revision surgery, so biomaterials based substitutes are still needed (8,11). The replacements currently used for this purpose are based on resorbable biological polymers, such as hyaluronic acid or fibrinogen, often releasing growth factors aimed at inducing in vivo cell migration from the remaining healthy tissues (12,13). As a consequence, the quality of these outcomes is highly related to the extent and morphology of the damage (14). Novel approaches for TM reconstruction giving rise to optimal acoustic function are highly desirable.

An advanced strategy to replace compromised tissues is offered by Tissue Engineering (TE).

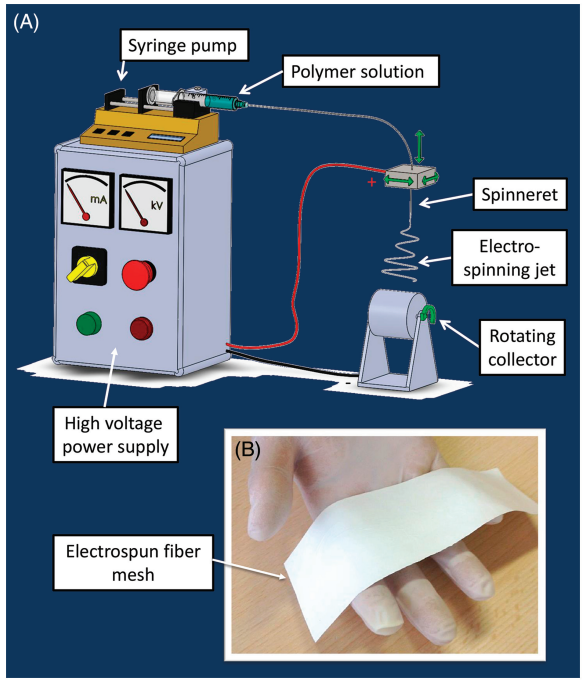


Figure 2. Electrospinning process and product. **(A)** Schematic drawing of the process, showing the necessary equipment and the principle of the method. **(B)** PEOT/PBT meshes as obtained after collection.

It relies on a combination of cells, three-dimensional (3D) porous materials (scaffolds), and suitable biochemical and/or physical factors, allowing differentiation and 3D arrangement of cells (15). If the tissue to be regenerated is sufficiently thin, like the TM, an in vitro approach is considered favourable. 3D scaffolds are usually necessary since in vitro cultured cells cannot organize themselves properly in a 3D architecture. Moreover, the material chemistry and topographic features may be strongly involved in determining cell viability, colonization, phenotype expression and extracellular matrix (ECM) molecule synthesis (16).

Electrospinning (ES) was developed for the textile industry in the first half of the last century. For its simplicity, versatility and cost-effectiveness, ES has recently gained a wide use in several fields, including biomedical scaffolding (17). The principle of the method exploits a fluid jet, usually a polymer solution, placed inside an electric field. Becoming electrically charged, the fluid out-sprout is accelerated towards the opposite polarity collector. While crossing the inter-pole distance, the liquid jet is stretched out and the solvent used for the preparation of the polymer solution starts to evaporate, giving rise to one ultrafine (i.e. with micron/submicron diameter) fibre that is finally collected in the form of a continuous non-woven mesh (18). An ES scheme is shown in Figure 2(A). The

maximum thickness of a mesh obtained via ES is usually a few hundred microns, after which the collected mesh acts as an insulator, preventing further fibre deposition. Therefore, ES is mostly suited to produce scaffolds replacing thin tissues or small lesions, such as skin and cartilage (19). This fabrication method may thus be ideal to produce scaffolds for TM replacement. In addition, it has been hypothesized by several authors that such ultrafine fibres emulate the behaviour of the fibrous ECM components, thus acting as biomimetic structures at the cell-material interface (20).

Several materials, including polymers and composites, have been electrospun with good results. Poly(ethylene oxide terephthalate)-*co*-poly(butylene terephthalate) (PEOT/PBT) multi-block copolymers are thermoplastic elastomers with good physical properties, including elasticity, strength and toughness, deriving from their phase-separated morphology, in which soft, hydrophilic PEO segments can physically cross-link in the presence of hard semi-crystalline PBT segments. This copolymer family has extensively been investigated for both in vitro and in vivo compatibility (21–23). Polyactive® is one among these copolymers currently approved for some clinical uses, e.g. as a stopper for orthopaedic surgery (24). Degradation of these copolymers occurs in aqueous media via hydrolysis and oxidation, with rates dependent on the PEOT/PBT ratio. In vivo studies have shown that macrophages are actively involved to remove degraded copolymer fragments via phagocytosis (25). For its characteristics, PEOT/PBT has been used to fabricate scaffolds for several applications, including skin, bone and cartilage. TM replacements based on this copolymer have also been reported in the literature. In the 1990s, PEOT/PBT salt-casted 100-μm-thick porous films were proposed as TM replacements. The authors described epithelial layers covering the implant, and only a mild foreign body reaction in a rat model (26–28). The failure experienced using alloplastic substitutes to replace the TM has been explained by the necessity to design the correct material topography and degradation rate (28). Consequently, with the onset of TE, otologists have started to look at synthetic materials with renewed emphasis (29). In a latest study, we have proposed ES in combination with a 3D fibre deposition via bioplotting to fabricate ex vivo TM substitutes with proper morpho-anatomic details (30). Those scaffolds were cultured in vitro for one week with human mesenchymal stromal cells (MSCs), as an immature cell model potentially able to develop the TM connective tissue. Moreover, although we have demonstrated that human MSCs colonized the surface of those scaffolds, cell infiltration inside the meshes was still to be improved in order to have full-thickness 3D cellular constructs appropriate for implantation. Interaction with TM keratinocytes is also required for formation of a functional eardrum.

This study is aimed at fabricating PEOT/PBT meshes as scaffolds for TM replacement using ES, with the intent to enable a TE approach suitable for eardrum perforations. The obtained scaffolds were morphologically analysed and cultured in vitro with human MSCs under dynamic flow regimen conditions, in order to enhance cell penetration within the fibres. The morphological features of human MSC/scaffold constructs were investigated in relation to those of the human TM using scanning electron microscopy and histochemistry. Cell adhesion, viability and scaffold colonization were studied. Finally, the capability of human tympanic keratinocytes to interact with the scaffold surface was tested.

New knowledge on the potential offered by ES in eardrum replacement could finally enable the translation of functional and biocompatible biohybrid TM constructs into clinical practice.

## Materials and methods

### *Fabrication of PEOT/PBT scaffolds*

Poly(ethylene oxide terephthalate)/poly(butylene terephthalate) (PEOT/PBT) segmented block copolymer was supplied by PolyVation BV (Groningen, The Netherlands). The copolymer used in this study was 300PEOT55PBT45. The commercial nomenclature aPEOTbPBTc represents: a is the molecular weight (Mw, $g \cdot mol^{-1}$) of the poly(ethylene glycol) (PEG); b and c are the weight ratios of PEOT and PBT, respectively. Chloroform ($CHCl_3$) was supplied by Merck KGaA (Darmstadt, Germany), hexafluorisopropanol (HFIP) by Biosolve BV (Valkenswaard, The Netherlands). The copolymer was dissolved in a solvent mixture of $CHCl_3$ and HFIP (90/10 v/v) to obtain a 20% w/v copolymer solution (31).

An ES apparatus was used to prepare ultrafine fibre meshes (Figure 2A). This apparatus is composed of a three-axis system (CNC-STEP, Germany) that allows the positioning and movement of the spinneret during the ES process. The system is also equipped with a syringe pump (KDS 100; KD Scientific, Holliston, MA, USA) to control the copolymer solution feed rate (F) and a high voltage power supply (Gamma High Voltage Research Inc., Ormond Beach, FL, USA) capable of generating up to 30 kV. The spinneret had a 21-gauge blunt tip and was positively charged. A grounded rotating drum collector with a 60-mm diameter and a 60-mm

length, with a 150 r.p.m. rotation velocity was used to produce randomly oriented meshes. The spinneret was translated collinearly to the rotating drum axis to produce a mesh with uniform thickness. The environment conditions inside the ES chamber, namely temperature ($25 \pm 1\,^{\circ}C$) and humidity (30%), were controlled by means of a custom-made ventilation system.

The mesh was finally collected after 30 min. After production, the PEOT/PBT scaffolds were treated with argon (Ar) plasma to improve cell adhesion by changing surface roughness (32). The scaffolds were placed inside a radio-frequency glow-discharge chamber (Harrick Scientific Corp., NY, USA). Thereafter, Ar gas was flushed for 30 min under controlled 0.1–0.2 mbar vacuum with high settings applied to the radio frequency coil (740 V DC, 40 mA DC, 29.6 W). The final electrospun product is shown in Figure 2(B).

*Scaffold characterization*

Scaffold morphology and the diameter of electrospun fibres were analysed via scanning electron microscopy (SEM). The scaffolds ($n = 2$) were mounted on aluminum stubs and sputter-coated with gold (Cressington, Watford, UK) prior to observation. SEM micrographs were obtained at different magnifications of the diverse regions of interest using a Phillips XL30 ESEM-FEG scanning electron microscope (Philips, Eindhoven, The Netherlands). Measurements of electrospun fibre diameters were performed via SEM over at least 100 fibres from randomly selected fields.

The scaffold porosity ($\varepsilon$) was obtained from the following formula (31):

$$\varepsilon = 1 - \rho \cdot \frac{M}{V}$$

In which $\rho$ is the density, $M$ the weight, and $V$ the volume of the fabricated scaffolds, measured with a pycnometer, a digital scale, and a digital micrometer (Mitutoyo Corp., Japan) for mesh thickness and area, respectively ($n = 3$).

Pore size distribution in the scaffolds ($n = 2$) was investigated via mercury intrusion porosimetry (MIP), using a Hg intrusion porosimeter equipped with a macropore unit (CE Instruments - ThermoQuest, Milano, Italy). The distribution of pore volumes was obtained from the derivative curve of the cumulative intruded volume, as a function of pore diameter, applying the Washburn equation:

$$d = 10 \cdot 4\gamma \cdot \cos\frac{\theta}{P}$$

This equation states that the diameter $d$ (μm) of the Hg-filled pores, assumed to be cylinders, is inversely proportional to the intrusion pressure P ($kg/cm^2$), if Hg surface tension $\gamma$ and contact angle $\theta$ between Hg and the material are constant.

The relative volumes of the pores were assigned to pore size classes and reported as relative volume percentages.

*Ethics statement*

The human TMs analysed in this study were collected from certified formalin-fixed cadaveric temporal bones, purchased from International Biologicals Inc. (Detroit, MI, USA). Isolation of human MSCs from bone marrow samples obtained during orthopaedic surgery was performed under approval of the Ethics Committee of Azienda Ospedaliero-Universitaria Pisana (Pisa, Italy).

Isolation of human keratinocytes was performed with approval from the St. John of God Healthcare Ethics Committee (Subiaco, Western Australia). Patients signed a written informed consent before the intervention and specimens were treated anonymously and in conformity with the principles and ethics standards expressed by the Declaration of Helsinki.

*Human MSC isolation*

Human MSCs were isolated from bone marrow aspirates, expanded and characterized as reported in our previous studies (33). Briefly, diluted bone marrow samples were layered on a density gradient (Lymphoprep; Axis-Shield, Norway), allowing the isolation of the mononuclear cells that were cultured in regular culture medium (CM), containing low-glucose (1 g/l) Dulbecco's Modified Eagle's Medium (D-MEM), 2 mM L-glutamine, 100 IU/ml penicillin and 100 mg/ml streptomycin (pen-strep) (all from Sigma-Aldrich) and supplemented with 10% (v%) heat-inactivated foetal bovine serum (FBS) (Invitrogen, Carlsbad, CA, USA). After 24 h, non-adherent cells were removed from the cultures through washing and the adherent cells were expanded up to reach about 70%–80% confluence. Cell cultures were carried out in an incubator under standard conditions, namely, $37\,^{\circ}C$, 95% relative humidity, and 5% $CO_2$/95% air environment.

*Human TM keratinocyte isolation*

Primary human TM-derived keratinocytes were grown from tissue explants and cultured as previously described (34). Briefly, human TM keratinocyte cultures were maintained in D-MEM supplemented with 4.5 g/l D-glucose (Gibco,

Australia), 10% FBS (Bovogen, Australia) and 1% pen-strep (Gibco) with CM changes every three days. Cells were passaged at 85% confluence. Cell cultures were carried out in a humidified incubator under standard conditions, as detailed above.

*Culture of human MSC/scaffold constructs*

The scaffolds were sterilized by soaking in absolute ethanol (Bio-Optica, Milan, Italy) overnight and rinsed three times for 10 min with 3 × pen-strep/antimycotics (Diflucan, from Pfizer-Italia, Latina, Italy) in sterile phosphate buffered saline (PBS) (Sigma-Aldrich, Milan, Italy). The samples were coated with a 2% gelatin (Type B, 75 Bloom, from bovine skin; Sigma-Aldrich) solution (w/v) in sterile filtered double-distilled water, removing excess gelatin solution before cell seeding.

Human MSCs, suspended in 2% gelatin solution, were seeded on the scaffolds at a density of 240,000 viable cells per $cm^2$ of scaffold surface. Human MSC/scaffold constructs were placed in multi-well plates and cultured using regular CM for one week. At this time-point, constructs were placed inside a bioreactor, and the cultures were continued for four more weeks.

The dynamic culture system (bioreactor) used in this study was a patented custom-made apparatus allowing the vertical oscillatory motion of the cell/scaffold samples in a CM filled tube at 0.23 Hz (PCT/IB2014/064593). The construct viability was monitored up to four weeks. At selected time-points, the samples were processed for morphological analyses, i.e. SEM, fluorescence microscopy, and histochemistry. Construct cultures, static and dynamic, were carried out in standard conditions.

*Culture of human TM keratinocyte/scaffold constructs*

PEOT/PBT electrospun discs, 7 mm in diameter, were placed into absolute ethanol overnight at room temperature and then washed in sterile PBS, pH 7.2 (Gibco, Australia) before coating in 2% gelatin (Sigma-Aldrich) PBS solution for 30 min. Excess gelatin was removed before cell seeding. Two control wells were coated with gelatin and two were left uncoated as tissue culture plastic (TCP) controls. Cell and construct cultures were performed inside 96-well plates in an incubator under standard culture conditions. Colonization assays were performed with human TM keratinocyte/scaffold constructs.

*Viability of human MSC/scaffold constructs*

The viability of the MSC/scaffold constructs was determined using non-disruptive colorimetric assays. The alamarBlue® assay (Serotec Ltd., Kidlington, UK). It was performed weekly to monitor the viability of the MSC/scaffold constructs and finally select the best culture time. Data were acquired according to the manufacturer's instructions and were expressed as percentage of reduced alamarBlue®. At the selected time-points, the dynamic cultures were temporarily stopped and the samples were placed in multi-well plates to perform the assay. Briefly, supernatants from samples ($n = 3$) and blank controls ($n = 3$) were incubated for 3 h at 37 °C with the dye/CM solution. For each test, 100 μl of supernatant from sample or control was loaded in 96-well plates and their absorbance was measured with a spectrophotometer (Victor 3; PerkinElmer, Waltham, MA, USA) under two wavelength readings (570 nm and 600 nm). Finally, the reduced alamarBlue® percentage was calculated correlating the absorbance values and the molar extinction coefficients of the dye at the selected wavelengths, following the manufacturer's protocol. After the assay, the samples were placed again in the bioreactor and the dynamic cultures were run again.

The Neutral Red (Sigma-Aldrich) assay was performed after two weeks to double-check the outcomes of the alamarBlue® assay. The constructs were incubated with 50 μg/ml of the dye in CM for 3 h, rinsed in sterile PBS and photographed with a digital camera (Canon Digital Ixus 50).

*Cell proliferation in human TM keratinocytes/scaffold constructs*

Cell proliferation was assessed using CellTitre 96® AQueous ONE Solution Cell Proliferation Assay (Promega Corporation, Australia). Briefly, a confluent monolayer of human TM keratinocytes was resuspended in 1 ml fresh D-MEM before seeding into control and test 96-wells at 10,000 cells per 0.1 ml. After 48 h, assay reagent was added for 2 h and then absorbance was measured on a Beckman Coulter AD200 spectrophotometer at a wavelength of 490 nm. Readings were made in duplicate, averaged and background corrected. Assays were conducted in duplicate wells and repeated three times ($n = 6$).

*SEM analysis*

SEM was used for a morphological evaluation of TMs and MSC/scaffold constructs. Human TMs ($n = 2$) were drawn from two formalin-fixed temporal bones via microdissection under surgical microscopy (OPMI microscope, Carl Zeiss, Oberkochen, Germany). Both biological and biohybrid (i.e. cell/scaffold) specimens were dehydrated in a graded series of ethanol aqueous solutions up to

absolute ethanol (Bio-Optica). To complete the dehydration, TM samples were treated with the critical point drying (Balzers CPD030; Oerlikon Balzers, Liechtenstein), while biohybrid constructs were dried in a vacuum oven at 37 °C overnight. Samples were mounted on aluminum stubs, sputter-coated with gold (Emitech K550), and observed via SEM (Jeol JSM-5200, and Zeiss EVO MA10).

*Histochemical analysis*

Histochemistry was performed on human MSCs, TMs and human MSC/scaffold constructs. Human MSCs grown on glass slides were fixed in 1% (w/v) buffered formalin at 4 °C for 10 min. TMs and biohybrid constructs (cultured for two weeks) were fixed in 4% (w/v) buffered formalin at 4 °C overnight, dehydrated through ethanol/water solutions and clarified in xylene at 40 °C. The 3D samples were embedded in paraffin at 60 °C. The sections were cut, deparaffinized and rehydrated before staining. The following histochemical analyses were performed on all the samples:

- haematoxylin and eosin (H&E), using a routine protocol, to evaluate cell morphology and cell infiltration in biohybrid constructs;
- periodic acid Shiff (PAS) reaction, for glycoprotein detection, was performed using a routine protocol; samples were counterstained with hematoxylin;
- Alcian Blue at pH 2.5, for glycosaminoglycan (GAG) detection. Briefly, Alcian Blue kit (Bio-Optica) was used according to the manufacturer's instructions. The samples were counterstained with 0.1% Nuclear Fast Red (Fluka, Buchs, Switzerland);

All the samples were dehydrated via ethanol/water series, clarified in xylene and mounted using a DPX mounting agent (Fluka) before observation under light microscopy (Leica Microsystems, Wetzlar, Germany).

*Fluorescence analysis*

After fixation, cell colonization in the biohybrid constructs was investigated via fluorescence microscopy. Due to the strong auto-fluorescence of the PEOT/PBT copolymer, the biohybrid constructs were soaked in 0.3% w/v Sudan black (Sigma-Aldrich)/70% ethanol solution for 1 h to reduce the background signal. The constructs were finally incubated with 4'-6'-diamidino-2-phenylindole, dihydrochloride (DAPI) fluorescent dye (Molecular Probes, Carlsbad, CA, USA), to visualize cell nuclei and detect cell distribution on the scaffold surface. Human MSC/scaffold constructs grown for four weeks were imaged with a Nikon Eclipse TE2000 inverted microscope. Fluorescence micrographs of human TM keratinocyte adhered to PEOT/PBT scaffolds were acquired from an Olympus BX60 microscope using a blue/cyan filter (Em/Ex 358/461nm) with a DP70 digital camera. Phase contrast micrographs were performed with a Moticam X WiFi camera (Motic, China) on a Nikon TS-100 inverted microscope.

*Statistical analysis*

In human/MSC scaffold constructs, quantitative data were presented as descriptive, mean ± standard deviation (SD), and inferential statistics ($p$-values). Statistical significance in the biochemical analyses was evaluated using the two-tailed $t$-test for either paired (alamarBlue assay and to observe cell localization®, intra-series comparisons) or unpaired (alamarBlue® assay and to observe cell localization, inter-series comparisons) data, followed by Bonferroni-Holm correction.

In human TM keratinocyte/scaffold constructs, quantitative data were presented as mean ± SD. Differences were analysed by analysis of variance (ANOVA) with post hoc $t$-test. Significance was set at $p < 0.05$.

## Results

*Scaffold morphology*

The processing parameters, optimized to produce uniform meshes and beadless fibres, are reported in Table I. After collecting the mesh under a rotating drum for 30 min, a uniform thickness was reached that enabled effective detachment from the collector and easy handling during the cell culture experiments. Thickness measurements, taken from three different meshes and three different regions within each mesh, were 220 ± 56 μm. SEM analysis showed that the produced electrospun meshes were composed of ultrafine randomly oriented fibres with 1.9 ± 0.9-μm diameter (Figure 3A). The scaffolds had 80% ± 0.8% porosity. MIP allowed pore size to

Table I. Processing parameters for the production of the electrospun mesh and obtained thickness and fibre diameter.

| | |
|---|---|
| Copolymer concentration | 20% v/v |
| Solvents $CHCl_3$/HFIP | 90/10 v/v |
| Applied voltage (kV) | 15 |
| Spinneret to collector (cm) | 15 |
| Feed rate (ml·h$^{-1}$) | 5 |
| Collector rotation (r.p.m.) | 150 |
| Collection time (min) | 30 |
| Fibre diameter (μm) | 1.9 ± 0.9 |
| Membrane thickness (μm) | 220 ± 56 |
| Porosity (%) | 80 ± 0.8 |

be evaluated and classified according to their diameters (Figure 3B). The macroporous meshes had about 96% of the void volume made by pores with 0.3–300-μm diameters. The 30–300-μm pore class, theoretically suitable for the migration of human MSCs, accounted for 19.7% of the relative volume, while the 3–30-μm pore class showed the highest value of 63.6%.

*TM characterization*

The micro-dissected TM samples showed good structural integrity. Two different areas were observed: a part very rich in collagen fibres (pars tensa) and a part containing low fibrillar components and a high quantity of amorphous matrix, fibroblasts and vascular channels (pars flaccida). The collagen fibres were well recognizable via SEM analysis (Figure 4A). In the histological specimens, it was possible to observe mucosal and squamous epithelia coating the TM on the inner and outer surfaces (Figure 4B). Both glycoproteins and GAGs were highly expressed and widely distributed in the connective tissue areas of the TMs (Figure 4C and D). To aid understanding of the histological panel, a schematic of the human TM cross-section, showing the trilaminar structure as described by Lim (1), is shown in Figure 1.

*Morphofunctional characterization of human MSCs*

After one week in culture, the MSCs showed spindle-like morphology and colony-forming capability (Figure 5A). The elongated morphology and basophilic cytoplasm of these cells was observed with H&E staining (Figure 5B). Cytochemical analyses confirmed the immature phenotype of these cells. Glycoproteins and GAGs were not detected at this stage of culture (Figure 5C and D).

*Viability of human MSC/scaffold constructs*

The alamarBlue® assay was performed on both static and dynamic biohybrid constructs up to four culture weeks (Figure 6A). The first week was conducted in static (traditional) culture, and showed no significant difference between the two groups of samples, being $32.35\% \pm 6.63\%$ and $31.41\% \pm 8.68\%$, respectively ($p = 0.6$, not significant). The further static culture of MSC/scaffold constructs lead to a reduced metabolic activity that was maintained through the

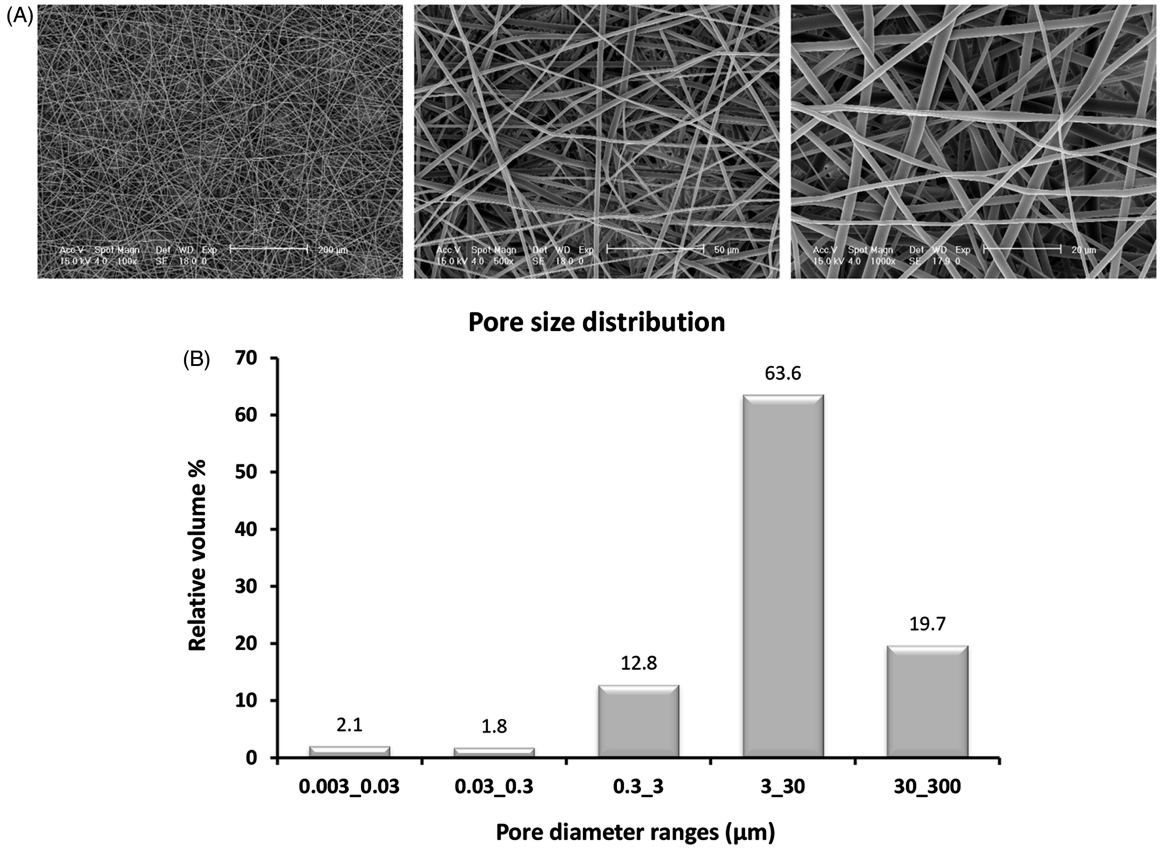


Figure 3. PEOT/PBT scaffold characterization. **(A)** Scanning electron micrographs showing the ultrafine fibre network at different magnifications (100×, 500× and 1000×). **(B)** Bar graph showing pore size distribution resulting from mercury intrusion porosimetry analysis. The assayed void volume was divided according to pore size classes and given as percentage.

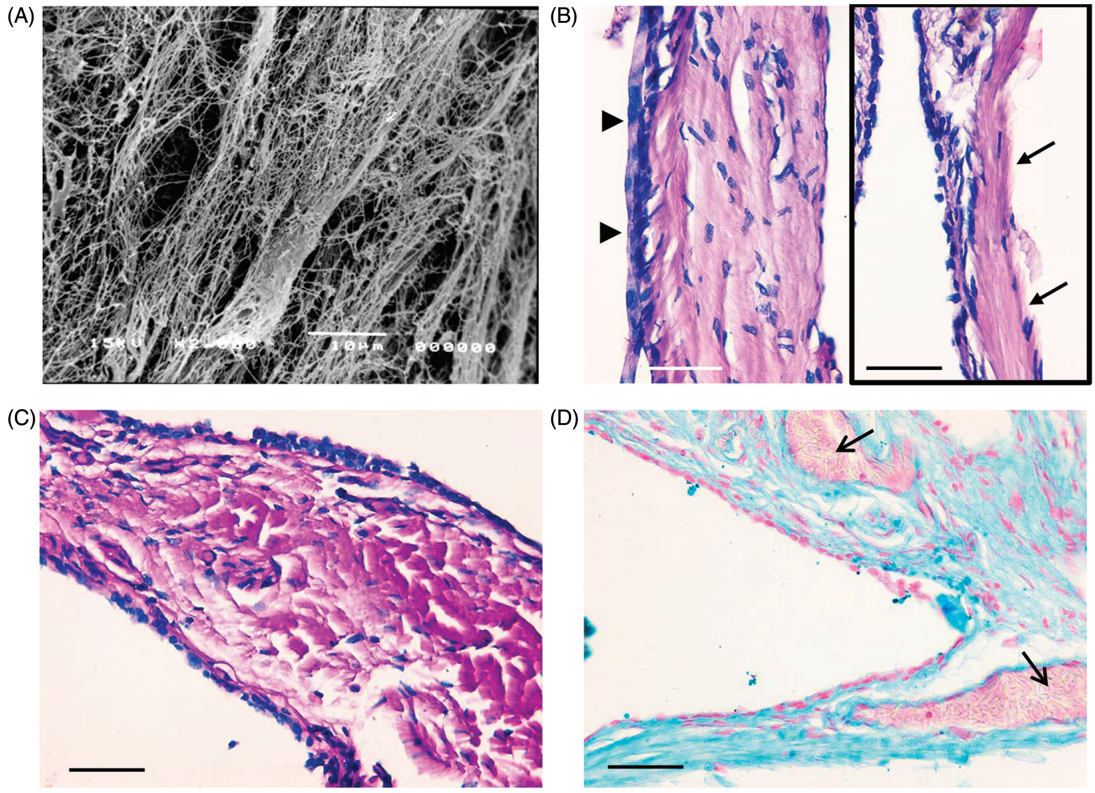


Figure 4. Characterization of human TM. **(A)** Scanning electron micrograph of the connective tissue layer showing collagen fibres. **(B–D)** Histologic analysis of TM cross-sections. **(B)** Composite image of H&E staining, showing tissue morphology. Arrows indicate the epidermal layer (detached from the connective layer upon processing), while arrowheads point out the mucosal epithelium. **(C)** PAS reaction of the pars flaccida, highlighting glycoproteins in pink. Cell nuclei are stained blue. **(D)** Alcian Blue staining at pH 2.5, revealing generic GAGs in cyan and cell nuclei in magenta. Arrows indicate blood vessels. **(B–D)** Scale bar is 50 μm.

whole culture. The alamarBlue® reduction was: $23.47\% \pm 1.01\%$, $28.11\% \pm 1.46\%$ and $24.47\% \pm 2.50\%$ at weeks 2, 3 and 4, respectively, with comparisons statistically significant, except those between weeks 1 and 3, and between weeks 2 and 4. In contrast, the cell viability was markedly increased in dynamic cultures. Specifically, the dye reduction percentages were: $64.48\% \pm 3.27\%$, $55.04\% \pm 1.32\%$ and $43.67\% \pm 2.55\%$, at weeks 2, 3 and 4, respectively, and all time-point comparisons showed statistically significant differences. Bioreactor cultures caused marked increases in cell metabolism compared to the static cultures at the same time-points. In comparisons of dynamic against static cultures, *p*-values were 0.0014, 0.000003, and 0.0004, at weeks 2, 3, and 4, respectively. After one week of dynamic culture (week 2), viability started to decline although remaining always superior to those of the static cultures. The highest viability gap was found at week 2.

The Neutral Red test was performed after two weeks in culture, namely, when the constructs reached the overall highest metabolic activity (i.e. $64.48\% \pm 3.27\%$ in the dynamic culture), as quantitatively evaluated with the alamarBlue® assay. This dye is internalized only by the viable cells and permitted their spatial distribution on the scaffold surfaces to be localized (Figure 6B and C). This assay showed the most intense staining in the samples cultured in dynamic conditions, thus confirming the results of the alamarBlue® assay. Moreover, the viable cells were uniformly distributed in the central areas of the discs, even if those in the bioreactor-cultured constructs appeared less organized in some areas (Figure 6C).

### *Morpho-functional analysis of human MSC/scaffold constructs*

Histological analysis performed after two weeks revealed that the static cultures gave rise to cells covering the fibre mesh as monolayers (Figure 7A). As a consequence of such a fragile interaction between the cells and the material, the cellular phase was often detached from the histological sections upon processing and could not be imaged. The morphological analysis performed on the human MSC/scaffold constructs could be best focused on samples cultured in the bioreactor.

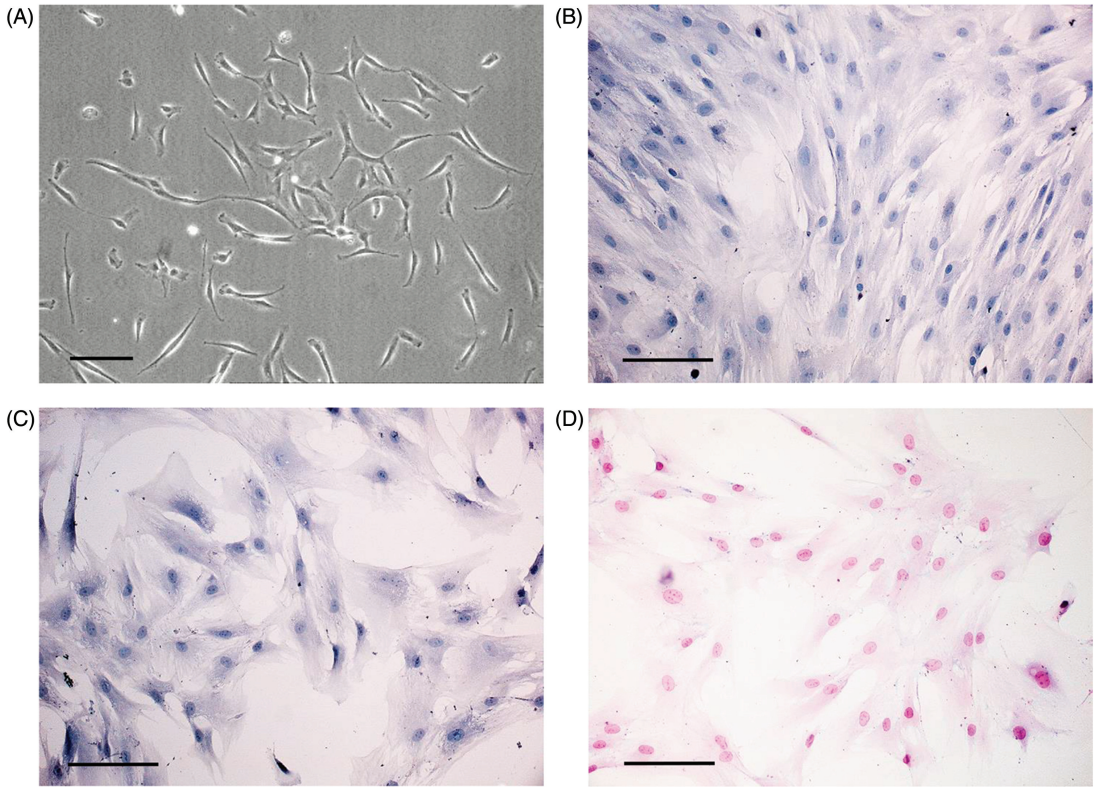


Figure 5. Characterization of human MSCs. **(A)** Phase contrast micrograph of cells one week after isolation (passage 1), highlighting spindle-shaped morphology. **(B–D)** Histological analysis of human MSCs cultured on glass slides for one week (passage 2). **(B)** H&E staining, showing basophilic cytoplasm. **(C)** PAS reaction is negative. Cell nuclei appear in blue. **(D)** Alcian Blue staining at pH 2.5 is negative. Cell nuclei are stained magenta. **(A–D)** Scale bar is 50 μm.



Under a dynamic flow culture regimen, the MSCs penetrated inside the mesh thickness up to $203 \pm 37$ μm and were well stretched out, as shown by H&E staining (Figure 7B). However, early levels of glycoproteins, synthesized only at intracellular level, could be detected (Figure 7D). Deposition of generic GAGs was almost negative (Figure 7F).

SEM analysis resulted helpful to image the constructs cultured in static conditions and showed cells disposed on the top surface of these scaffolds attached to the copolymer fibres after two weeks in culture (Figure 7C). The surface colonization of these constructs was confirmed by fluorescence microscopy analysis after four weeks, which showed intact nuclei without chromatin condensation (Figure 7E).

### *Characterization of human TM keratinocyte/scaffold constructs*

When seeded with human TM keratinocytes, the cells were noted to adhere to the scaffold and remained viable at the 48 h endpoint of the assay. Appreciable numbers of cells were retained on the scaffolds over the short-term culture, although after initially plating the same cell number in control and test wells, numbers were less on the test scaffold than on plastic or gelatin-coated plastic controls by 48 h (Figure 8A). The control wells contained confluent tightly packed monolayers of cells with typical cobblestone morphology (Figure 8B). The opaque materials meant that it was not possible to image by routine phase contrast microscopy (Figure 8C); however, with fluorescence microscopy the test scaffolds were shown to have cells adherent to the upper surface of the scaffold with an even distribution, aside from some cell loss due to handling artefacts (Figure 8D). Higher magnification showed healthy cell nuclei with no evidence for apoptosis or necrosis and no evidence for any substantial migration into the deeper layers of the electrospun scaffold (Figure 8E).

## Discussion

TE has recently been invoked by ear scientists as a valuable approach to develop alternatives to the current TM replacements in otosurgery (29,35). In reconstructive surgery, the availability of tissues for autografting may be insufficient and the implant of alloplastic materials is controversial (36). As a consequence, an ideal TM substitute is still the

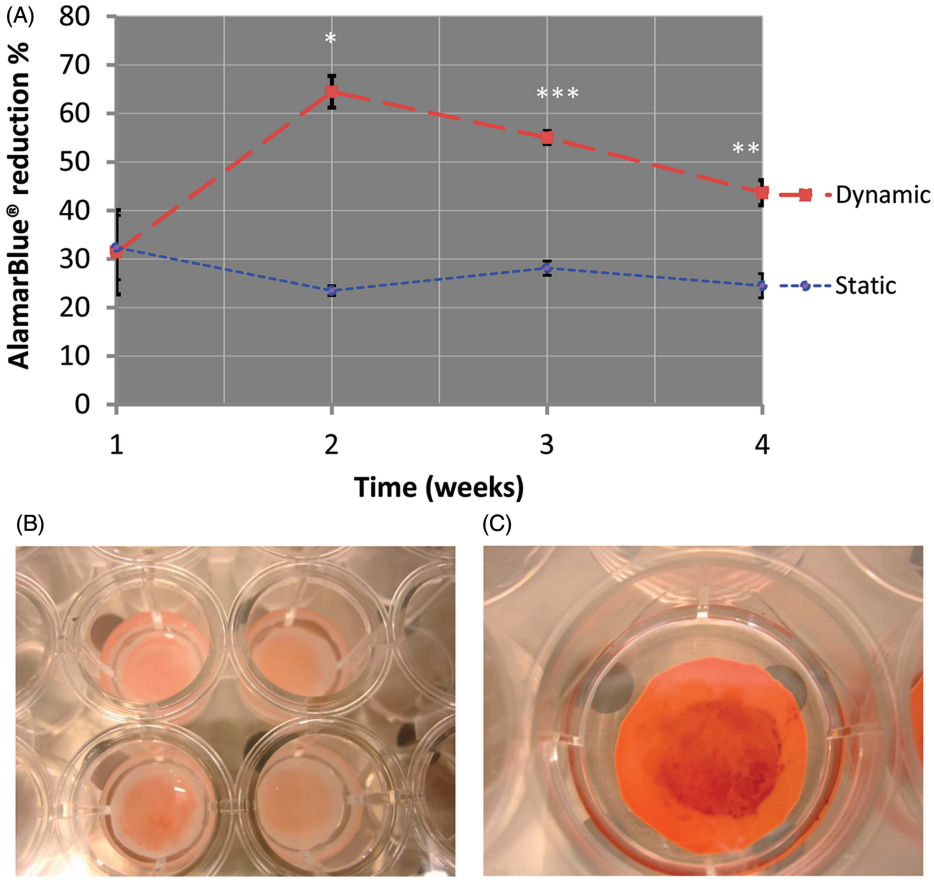


Figure 6. Viability of human MSC/scaffold constructs comparing static versus dynamic culture conditions. **(A)** Bar graph showing the results of the alamarBlue® assay up to four weeks. *p*-values are: *0.0014, ***0.000003, and **0.0004. **(B,C)** Photographs showing the Neutral Red uptake after two weeks in culture. **(B)** Samples cultured under static (traditional) conditions. **(C)** Sample cultured in the bioreactor (dynamic conditions).

subject of investigation. Since the last century, synthetic biomaterial devices have been conceived by otologists as mere prosthetic replacements or, in the specific case of the eardrum, as sheeting substrates promoting TM self-repair via endogenous cell migration (25–27). From a TE perspective, the replacement is a functional biohybrid construct, which means a fully integrated cell/scaffold material. Such cellularized 3D materials may be preliminarily generated in vitro and may thereafter complete differentiation in vivo, while interacting with the physiological microenvironment. For TE applications, the biomaterials, usually processed to form porous bio-resorbable structures to be colonized by autologous cells, should disappear over a time proper for neo-tissue development and connection with vasculature and surrounding tissues (15). ES is one of the most widespread and easily accessible scaffolding techniques by most biomaterials laboratories that could promote relevant advances in eardrum repair (30). The underlying rationale for the generation of tissue-engineered TM substitutes via ES relies on the morpho-structural features of these fibre meshes that recall the shape and size of a thin connective tissue layer, thus appearing particularly suitable to replace the lamina propria of the TM.

This study is aimed at investigating electrospun scaffolds to replace the fibrous layer of the eardrum, using an in vitro approach driven by TE concepts. A copolymer of the PEOT/PBT family was chosen to prepare ultrafine fibre meshes via ES, as a model of FDA approved synthetic material. Some studies performed at the end of the last century in the Netherlands have proposed this copolymer family for middle ear applications due to the customizable degradation times and evidence of very mild inflammatory reaction after in vivo implantation (25–27).

In our recent study, we have reported on the use of ES in combination with 3D fibre deposition, the latter as an advanced manufacturing technique, to produce PEOT/PBT scaffolds for the TM (30). These scaffolds were designed to show directional macro-scaled pathways mimicking the radial and circular morphology of collagen fibres in the lamina propria of the pars tensa. The electrospun layer in

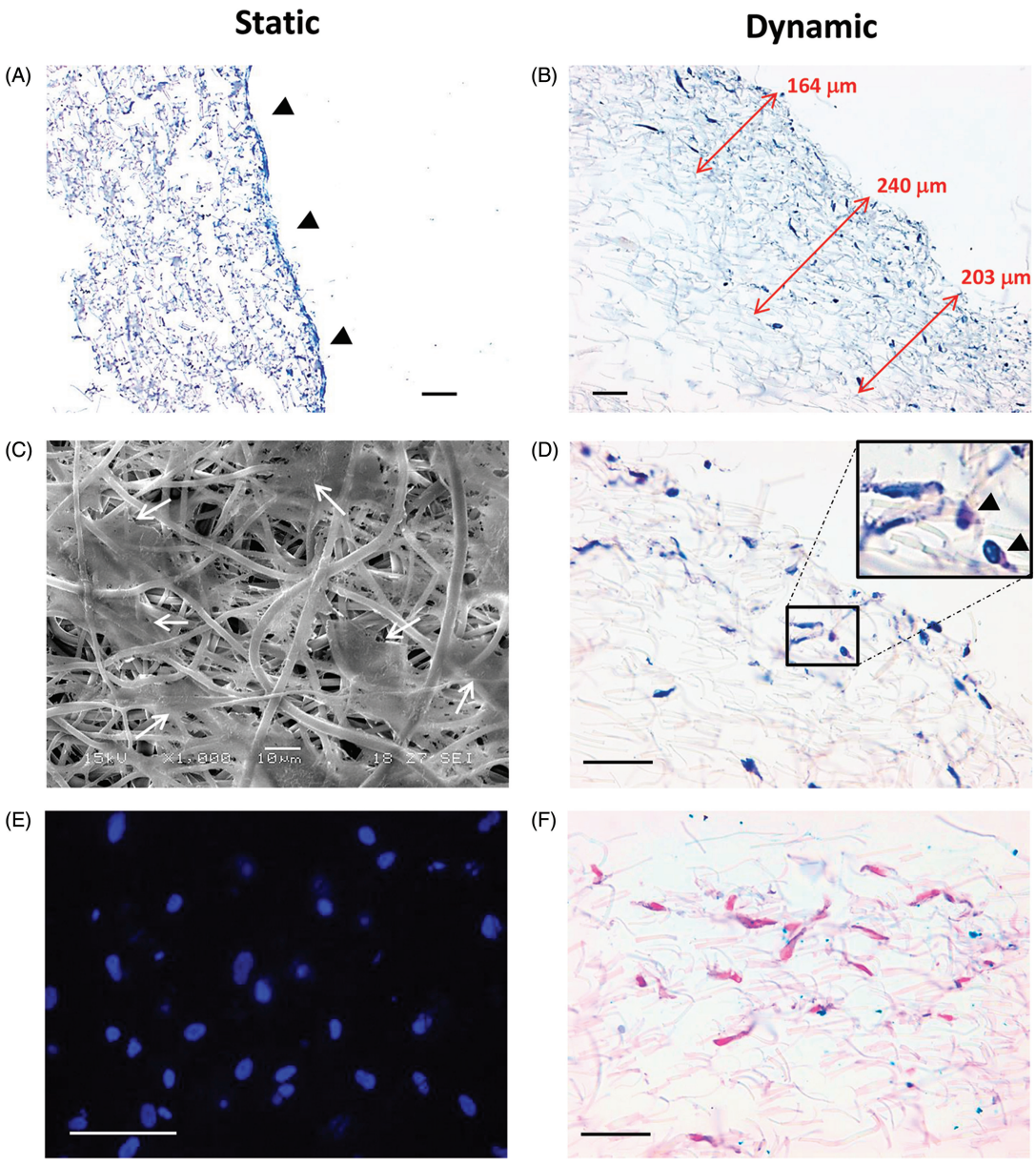


Figure 7. Morpho-functional analysis of human MSC/scaffold constructs after two weeks. **(A,C,E)** Results of samples cultured in well-plates (under static conditions). **(B,D,F)** Results of samples cultured in the bioreactor (under dynamic conditions). **(A,B)** H&E staining of cross-sectioned constructs. **(A)** Arrowheads show a cell monolayer on the top surface of the scaffold. **(B)** Double arrows indicate cell penetration into the mesh thickness with respect to the scale bar. **(C)** Scanning electron micrograph of the top surface of the cell/scaffold construct. Arrows indicate cells interacting with the mesh fibres. **(D)** PAS reaction, showing low production of glycoproteins (in pink). Cell nuclei are in blue. Magnified insets highlight intracellular PAS positivity. **(E)** Fluorescence micrograph of DAPI stained cell nuclei on the top surface of the scaffold. **(F)** Alcian Blue staining at pH 2.5 showing lack of GAG production. Cell nuclei are in magenta. **(A,B,D–F)** Scale bar is 50 µm.

such scaffolds was very thin (<50 µm), and difficult to handle for surgery and culture in vitro in the absence of a rigid frame, like the one provided by 3D fibre deposition.

In this study, we used ES alone to fabricate thicker meshes than those previously assayed in order to be able to test them in dynamic flow culture conditions. After fabrication, the PEOT/PBT copolymer meshes showed a very consistent and reproducible morphology. The electrospun scaffolds had fibre diameter of $1.9 \pm 0.9$ µm and mesh thickness of $220 \pm 56$ µm. The mesh porosity was $80\% \pm 0.8\%$. The macroporous materials were theoretically suitable for 3D cell colonization, since 83.3% of relative void volume was in pores of 3–300-µm size. The capability of cell penetration in porous structures depends on the size and migratory attitude of each different cell type. As an example,

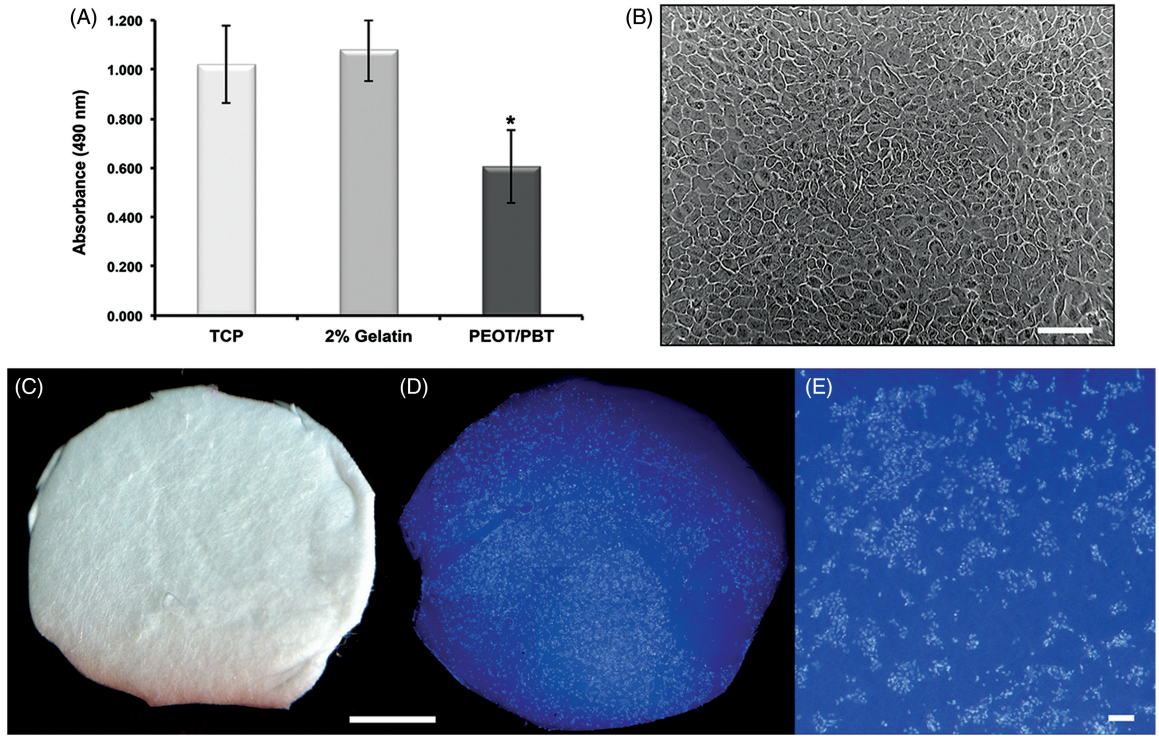


Figure 8. Human tympanic membrane keratinocytes interacting with PEOT/PBT electrospun scaffolds. **(A)** Bar graph showing colorimetric assay for viable cells on culture well plastic, gelatin-coated TCP and gelatin-coated PEOT/PBT scaffolds at 48 h after plating. *<0.05. **(B)** Phase contrast micrograph of human tympanic membrane keratinocytes. **(C)** Photograph of a scaffold. **(D,E)** Human tympanic membrane keratinocytes stained with DAPI to show cell adhesion and distribution on the scaffold. **(E)** Higher magnification of **(D)**. Scale bar is: 100 μm for **(B,E)**, 2mm for **(C,D)**.

human MSCs are known to be large cells with dimension up to a hundred microns, which may encounter difficulties in penetrating electrospun fibre networks (30). For these cells, the pore size actually usable will most probably be in the 30–300-μm range, which in our materials accounts for only 19.7% of the relative void volume. Finally, it has to be noted that the pores in these fibrous scaffolds do not have typical cylinder or sphere shapes. Therefore, cell infiltration inside electrospun meshes has usually been reported to show some limitations due to the strongly interlaced arrangement of the fibrous polymer network that may be arduous to penetrate at the cell-scale level. To overcome this issue, flow perfusion bioreactor systems have been applied in some TE studies, demonstrating that cell infiltration is also affected by the thickness of the fibre layer (37).

In this study we used a custom-made bioreactor able to move the culture inside the CM at a frequency of 0.23 Hz. This cyclic motion may be more biomimetic for growing TM replacements than unidirectional stream motions, like those provided by flow perfusion bioreactors (37). In our strategy, immature cells, like MSCs, could be used to generate autologous cell/scaffold constructs replacing the lamina propria of the eardrum, which can eventually complete differentiation in vivo by exploiting the microenvironment stimuli. The application of stem cells in TM perforations, without scaffolding material, was first proposed by Rahman et al. and documented in a rat model (38). From embryology, the TM mid-layer originates from the branchial arch mesenchyme, a connective-like tissue derived from the mesoderm. Bone marrow MSCs are adult undifferentiated immature cells of mesoderm origin retaining fibroblast morphology and capable of self-renewal and multipotency (39). For all these reasons, and envisioning a product translation from bench to bedside, human MSCs were chosen as a cellular model for TM reconstruction (30). A TM biopsy to isolate TM autologous fibroblasts may be not possible or not recommended in patients affected by eardrum perforations or middle ear infections. At the starting point, the copolymer ultrafine fibres are supposed to mimic the topographical properties of native ECM and provide structural strength. Thereafter, upon culture and final implantation, the MSCs could differentiate into TM fibroblasts thanks to appropriate physiochemical stimuli leading to the production of ECM molecules, including collagen fibres, which will

replace the degrading copolymer network. The presence of non-epithelial cells, capable of differentiation and showing fibroblastic features, such as MSCs, can play a determining role in the regeneration of a functional TM. The closure of a TM perforation is typically driven by epithelial migration, which occurs easily in vivo (40). However, the self-healed area of a perforated TM can lack the lamina propria layer. As a consequence, the bilaminar eardrum shows sub-optimal acoustic ability, enhanced susceptibility to retraction pocket formation and increased vulnerability to re-perforation for minor barotraumas (35). The formation of a trilaminar structure resembling the native eardrum is a primary goal of TM replacement strategies, with the mid-layer being the most critical to regenerate.

We demonstrated that bioreactor culture increased the viability of human MSCs in the scaffolds compared to the traditional multi-well plate cultures at all the time-points. The highest viability gap between these culture groups was found after one week in dynamic flow culture conditions. Subsequently, this difference started to be reduced, although remaining always superior, with statistical significance, in dynamic conditions. In static cultures, the viability ranged from $32.35\% \pm 6.63\%$ at the beginning, to $24.47\% \pm 2.50\%$ at endpoint, showing an averagely constant trend. The time-point at which the highest viability was reached ($64.48\% \pm 3.27\%$ in dynamic culture conditions) was thus selected to perform morphological and histochemical analyses to determine human MSC infiltration and differentiation induced by mechanical stimuli. No differentiating supplements were added in the CM. In static cultures, the human MSCs interacted with the fibrous scaffold mainly on the top surface. This phenomenon was also described in our previous study (30). In that case, the electrospun thickness was about five times lower than the one tested here, and some human MSCs penetrating the mesh thickness were observed (30,37). Differently, the dynamic flow regimen forced the cells to infiltrate into the mesh thickness up to 240-μm depth, a thickness almost comparable with the minimum thickness of the mesh. It is also important to point out that the pore classes poorly suitable for cell infiltration ($<30\,\mu m$) concur with metabolite and catabolite diffusion, playing an important role in maintaining cell viability in the inner areas of the scaffolds. This is of crucial importance in dynamic conditions, if cells penetrate to a relevant distance to the surfaces and cannot easily access nutrients. The human MSCs cultured in the bioreactor on PEOT/PBT scaffolds maintained a non-differentiated phenotype, as shown by very low production of GAGs and glycoproteins, which are conversely highly expressed in the eardrum connective layer. This evidence indicates that the mechanical stimuli alone, as applied in our bioreactor, were not sufficient to induce ECM production after one week. Further studies should be focused on differentiation protocols, enabling at least an initial maturation of the biohybrid TM constructs to be completed in vivo.

The last step of our study was to assess an efficient interaction between the PEOT/PBT electrospun scaffolds and human TM keratinocytes, as a model of in vivo epithelial response (34). The outer lining of the TM is made up of a keratinizing epithelium that protects the eardrum from physical and chemical insults (1,35). From our experiments, the human TM keratinocytes adhered to the scaffold surfaces and were found viable and well spread out 48 h after seeding. Longer-term experiments were beyond the scope of the current study, but repopulation kinetics for the outer and inner TM surface and interaction of human MSCs and TM keratinocytes with these electrospun scaffolds are valid for further investigations.

Altogether, the obtained findings confirmed the high potential of electrospinning in developing TM substitutes using TE approaches. In particular, a biohybrid fibrous mid-layer could be generated in vitro, while the epithelia could migrate in vivo covering the replacements. Trilaminar biohybrid constructs could be a valuable option to repair perforated eardrums that in our opinion deserve further research.

## Conclusion

This study shows the possibility to generate trilaminar biohybrid replacements of TM via a TE approach. Specifically, fibrous scaffolds were produced via ES using PEOT/PBT as an FDA-approved copolymer that gave promising results in middle ear applications. Human MSCs derived from the bone marrow were used as a cellular model of giving rise to fibroblastic differentiation with production of ECM molecules replacing the TM connective tissue layer. Full thickness cell/scaffold constructs were generated using a bioreactor. However, under the tested conditions, the human MSCs maintained an uncommitted phenotype. Finally, human TM keratinocytes demonstrated a good interaction with the scaffolds, suggesting their capability of being covered by the native epithelia. Subsequent studies should focus on protocols for addressing MSC differentiation into TM fibroblasts, in order to apply functional TM replacements to the patients.

## Acknowledgements

This study was supported by the Tuscany Region (Health Program 2009) and by the Italian Ministry of University and Research (PRIN 2010S58B38). Sabrina Danti (University of Pisa) is gratefully acknowledged for contributing to statistical analysis.

## Declaration of interest

The authors declare that there are no conflicts of interest.



## References

1. Lim DJ. Structure and function of the tympanic membrane: a review. Acta Otorhinolaryngol Belg. 1995;49:101–15.
2. Fay J, Puria S, Decraemer WF, Steele C. Three approaches for estimating the elastic modulus of the tympanic membrane. J Biomech. 2005;38:1807–15.
3. Monasta L, Ronfani L, Marchetti F, Montico M, Vecchi Brumatti L, Bavcar A, et al. Burden of disease caused by otitis media: systematic review and global estimates PLoS One. 2012;7:e36226.
4. Mehta RP, Rosowski JJ, Voss SE, O'Neil E, Merchant SN. Determinants of hearing loss in perforations of the tympanic membrane. Otol Neurotol. 2006;27:136–43.
5. Morris P, Leach A, Silberberg P, Mellon G, Wilson C, Hamilton E, et al. Otitis media in young aboriginal children from remote communities in Northern and Central Australia: a cross-sectional survey. BMC Pediatr. 2005;5:27.
6. Louw L. Acquired cholesteatoma pathogenesis: stepwise explanations. J Laryngol Otol. 2010;124:587–93.
7. Aggarwal R, Saeed S, Green K. Myringoplasty. J Laryngol Otol. 2006;120:429–32.
8. Feenstra L, Kohn FE, Feyen J. The concept of an artificial tympanic membrane. Clin Otolaryngol Allied Sci. 1984;9:215–20.
9. Kerr AG. Homografts in the middle ear. J R Soc Med. 1980;73:610.
10. Dornhoffer JL. Hearing results with cartilage tympanoplasty. Laryngoscope. 1997;107:1094–9.
11. Kaftan H. Tympanic membrane reconstruction with non-autogenous transplants and alloplastic materials. Laryngorhinootologie. 2010;89:562–8.
12. Ozturk K, Yaman H, Avunduk MC, Arbag H, Keles B, Uyar Y. Effectiveness of MeroGel hyaluronic acid on tympanic membrane perforations. Acta Oto-Laryngologica. 2006;126: 1158–63.
13. Kanemaru S, Umeda H, Kitani Y, Nakamura T, Hirano S, Ito J. Regenerative treatment for tympanic membrane perforation. Otol Neurotol. 2011;32:1218–23.
14. Lou ZC, Lou ZH, Zhang QP. Traumatic tympanic membrane perforations: a study of aetiology and factors affecting outcome. Am J Otolaryngol. 2012;33:549–55.
15. Langer R, Vacanti JP. Tissue Engineering. Science. 1993;260:920–6.
16. MacArthur BD, Oreffo RO. Bridging the gap. Nature. 2005;433:19.
17. Pham QP, Sharma U, Mikos AG. Electrospinning of polymeric nanofibres for tissue engineering applications: a review. Tissue Eng. 2006;12:1197–211.
18. Shin YM, Hohman MM, Brenner MP, Rutledge GC. Electrospinning: a whipping fluid jet generates submicron polymer fibres. Appl Phys Lett. 2001;78:1149.
19. Kumbar SG, James R, Nukavarapu SP, Laurencin CT. Electrospun nanofibre scaffolds: engineering soft tissues. Biomed Mater. 2008;3:034002.
20. James R, Toti US, Laurencin CT, Kumbar SG. Electrospun nanofibrous scaffolds for engineering soft connective tissues. Methods Mol Biol. 2011;726:243–58.
21. Beumer GJ, van Blitterswijk CA, Ponec M. Degradation behaviour of polymeric matrices in (sub)dermal and muscle tissue of the rat: a quantitative study. Biomaterials. 1994;15:551–9.
22. Beumer GJ, van Blitterswijk CA, Ponec M. Biocompatibility of degradable matrix induced as a skin substitute: an in vivo evaluation. J Biomed Mater Res. 1994;28:545–52.
23. Mensik I, Lamme EN, Riesle J, Brychta P. Effectiveness and safety of the PEGT/PBT copolymer scaffold as dermal substitute in scar reconstruction wounds (feasibility trial). Cell Tiss Bank. 2002;3:245–53.
24. Bulstra SK, Geesink RG, Bakker D, Bulstra TH, Bouwmeester SJ, van der Linden AJ. Femoral canal occlusion in total hip replacement using a resorbable and flexible cement restrictor. J Bone Joint Surg Br. 1996;78:892–8.
25. Bakker D, van Blitterswijk CA, Hesseling SC, Grote JJ, Deams WT. Effect of implantation site on phagocyte/polymer interaction and fibrous capsule formation. Biomaterials. 1988;9:14–21.
26. Bakker D, van Blitterswijk CA, Hesseling SC, Koerten HK, Kuijpers W, Grote JJ. Biocompatibility of a polyether urethane, polypropylene oxide, and a polyether polyester copolymer. A qualitative and quantitative study of three alloplastic tympanic membrane materials in the rat middle ear. J Biomed Mater Res. 1990;24:489–515.
27. Bakker D, van Blitterswijk CA, Hesseling SC, Th. Daems W, Kuijpers W, Grote JJ. The behaviour of alloplastic tympanic membranes in Staphylococcus aureus-induced middle ear infection. I. Quantitative biocompatibility evaluation. J Biomed Mater Res. 1990;24:669–88.
28. Grote JJ, Bakker D, Hesseling SC, van Blitterswijk CA. New alloplastic tympanic membrane material. Am J Otol. 1991;12:329–35.
29. Teh BM, Marano RJ, Shen Y, Friedland PL, Dilley RJ, Atlas MD. Tissue engineering of the tympanic membrane. Tissue Eng. Part B. 2013;19:116–32.
30. Mota C, Danti S, D'Alessandro D, Trombi L, Ricci C, Puppi D, et al. Multiscale fabrication of biomimetic scaffolds for tympanic membrane tissue engineering. Biofabrication. 2015;7:025005.
31. Moroni L, Licht R, de Boer J, de Wijn JR, van Blitterswijk CA. Fibre diameter and texture of electrospun PEOT/PBT scaffolds influence human mesenchymal stem cell proliferation and morphology, and the release of incorporated compounds. Biomaterials. 2006;27:4911–22.
32. Woodfield TB, Miot S, Martin I, van Blitterswijk CA, Riesle J. The regulation of expanded human nasal chondrocyte re-differentiation capacity by substrate composition and gas plasma surface modification. Biomaterials. 2006; 27:1043–53.
33. Trombi L, Mattii L, Pacini S, D'Alessandro D, Battolla B, Orciuolo E, et al. Human autologous plasma-derived clot as a biological scaffold for mesenchymal stem cells in treatment of orthopaedic healing. J Orthop Res. 2008;26:176–83.

34. Ghassemifar R, Redmond S, Zainuddin, Chirila TV. Advancing towards a tissue-engineered tympanic membrane: silk fibroin as a substratum for growing human eardrum keratinocytes. J Biomater Appl. 2010;24:591–606.
35. Hong P, Bance M, Gratzer PF. Repair of tympanic membrane perforation using novel adjuvant therapies: a contemporary review of experimental and tissue engineering studies. Int J Pediatric Otorhinolaryngol. 2013;77:3–12.
36. Dormer KJ, Gan RZ. Biomaterials for implantable middle ear hearing devices. Otolaryngol Clin North Am. 2001;34:289–97.
37. Pham QP, Sharma U, Mikos AG. Electrospun poly(epsilon-caprolactone) microfibre and multilayer nanofibre/microfibre scaffolds: characterization of scaffolds and measurement of cellular infiltration. Biomacromolecules. 2006;7:2796–805.
38. Rahman A, Olivius P, Dirckx J, Von Unge M, Hultcrantz M. Stem cells and enhanced healing of chronic tympanic membrane perforation. Acta Otolaryngol. 2008;128:352–9.
39. Mallo M. Embryological and genetic aspects of middle ear development. Int J Dev Biol. 1998;42:11–22.
40. Johnson AP, Smallman LA, Kent SE. The mechanism of healing of tympanic membrane perforations. Acta Otolaryngol. 1990;109:406–15.